

Formation of Palladium Nanostructures in a Seed-Mediated Synthesis through an Oriented-Attachment-Directed Aggregation

Laure Bisson,^{†,‡} Cedric Boissiere,[†] Lionel Nicole,[†] David Grosso,[†] Jean Pierre Jolivet,[†] Cécile Thomazeau,[‡] Denis Uzio,[‡] Gilles Berhaut,[§] and Clément Sanchez^{*,†}

[†]Laboratoire de Chimie de la Matière Condensée de Paris, Université Pierre et Marie Curie, Paris 6, CNRS, 4 place Jussieu, 75252 Paris cedex 05, France, [‡]IFP-Lyon, IFP, BP3, 69390 Solaize, France, and [§]Institut de Recherches sur la Catalyse et l'Environnement de Lyon, UMR 5256 CNRS-Université Lyon I, 2 avenue Albert Einstein, 69100 Villeurbanne, France

Received December 18, 2008. Revised Manuscript Received May 4, 2009

In the present article, we studied the structuration mechanism of palladium nanocrystals (NCs) of different shapes (cubes, pentatwinned nanorods, pyramids, and pentatwinned decahedra) prepared via the seed-mediated reduction of a palladium salt in aqueous medium, in the presence of CTAB surfactant. A detailed time-resolved TEM kinetic study of the formation of the NCs and the investigation of the influence of seeds size the characteristics of the final particles were performed. At the opposite of the gold reference synthesis reported in literature, the systematic presence of numerous very small palladium spherical nuclei generated by homogeneous nucleation was observed. A formation mechanism was proposed, taking into account an early aggregation step of the preformed seeds with some nuclei; this led to the formation of secondary objects with nonrandom shapes, the growth of which led eventually to the final well-faceted palladium NCs. An oriented attachment of seeds and nuclei, triggered by the energetically most favorable packing of spheres, was found to be responsible for the early differentiation of NCs shapes. The original formation mechanism presented here shed a new light on the seed-mediated synthesis of palladium NCs by (i) explaining shape differentiations via an oriented attachment process and (ii) explaining in detail the influence of the CTAB surfactant, the seed size on nuclei size ratio, the solvent, and the temperature onto final NCs shapes.

Introduction

Materials science researchers have for a long time been interested in mastering crystal sizes and shapes. Up to the end of the 1990s, the scientists' consensus reported in teaching books was that the bottom-up synthesis of crystals was dominated by a simple mechanism consisting of a nucleation step followed by a growth step, both being controlled by a few parameters, mainly saturation of the precursor solution, cohesive energy of bulk, and surface energies of particles.^{1,2} With the arising of nanotechnology in materials science, the need for colloidal nanoparticles as functional building blocks with specific properties led to the development of various synthesis procedures (coprecipitation, solvothermal–hydrothermal, reversed micelles syntheses, etc.), allowing the kinetic control of nanocrystals (NC) size, shape, and anisotropy. In these methods, nucleation and crystal surface energy are finely tuned via the preferential adsorption of some chemical additives onto

specific crystallographic facets.^{3–11} Although the morphology control achieved by this method is qualitative and empiric in many cases, some specific systems such as metal-oxide NCs (titanium, iron, and aluminum oxides, for example) grown in aqueous media could be described by consistent theoretical models predicting the morphological variations of these NCs as a function of the pH and the variation of surface energy of the different crystallographic facets stabilized by inorganic ions or organic additives.^{12–14}

Alternatively, extensive efforts have been devoted to the synthesis of noble metallic NCs. Since the first legendary synthesis of Turkevitch et al.,¹⁵ gold and, at a minor scale, silver metal NC syntheses in solution have been extensively described. Moreover, they are easy to prepare and exhibit very interesting electronic properties depending on their size

*Corresponding author. E-mail: clement.sanchez.upmc.fr.

- (1) Mesocrystals and Nonclassical Crystallization; Cölfen, H., Antonietti, M., Eds.; Wiley: Chichester, U.K., 2008; p 276.
- (2) Wulff, G. Z. *Krystallogr.* **1901**, *34*, 449.
- (3) Bradley, J. S.; Hill, E. W.; Klein, C.; Chaudret, B.; Duteil, A. *Chem. Mater.* **1993**, *5*(3), 254–256.
- (4) Chaudret, B. C. R. *Phys.* **2005**, *6*(1), 117–131.
- (5) Pileni, M. P. *Nat. Mater.* **2003**, *2*(3), 145.
- (6) Pileni, M. P. *J. Exp. Nanosci.* **2006**, *1*(1–4), 13–27.
- (7) Pastoriza-Santos, I.; Liz-Marzan, L. M. *Nano Lett.* **2002**, *2*(8), 903–905.

- (8) Perez-Juste, J.; Pastoriza-Santos, I.; Liz-Marzan, L. M.; Mulvaney, P. *Coord. Chem. Rev.* **2005**, *249*(17–18), 1870–1901.
- (9) Manna, L.; Scher, E. C.; Alivisatos, A. P. *J. Am. Chem. Soc.* **2000**, *122*(51), 12700–12706.
- (10) Yin, Y.; Alivisatos, P. *Nature* **2005**, *437*, 664–670.
- (11) Thomson, T.; Toney, M. F.; Raoux, S.; Lee, S. L.; Sun, S.; Murray, C. B.; Terris, B. D. *J. Appl. Phys.* **2004**, *31*(5/6), 149–156.
- (12) Jolivet, J. P.; Cassaignon, S.; Chaneac, C.; Chiche, D.; Tronc, E. *J. Sol–Gel Sci. Technol.* **2008**, *46*, 299–305.
- (13) Jolivet, J. P.; Froidefond, C.; Pottier, A.; Chaneac, C.; Cassaignon, S.; Tronc, E.; Euzen, P. *J. Mater. Chem.* **2004**, *14*, 3281–3288.
- (14) Vayssieres, L.; Chaneac, C.; Tronc, E.; Jolivet, J. P. *J. Colloids Interface Sci.* **1998**, *205*(2), 205–212.
- (15) Turkevich, J.; Stevenson, P. C.; Hillier, J. *Discuss. Faraday Soc.* **1951**, *11*, 55.

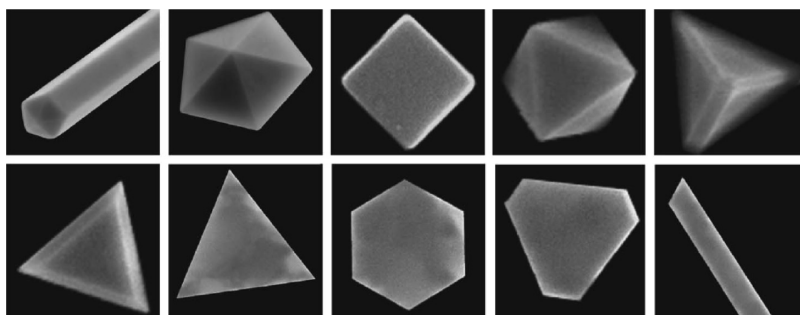


Figure 1. SEM images of the most characteristic morphologies: pentagonal cross-section nanowires, decahedral particles, cubic particles, octahedral particles, tetrahedral and truncated tetrahedral particles, and platelets with different shapes. Reprinted with permission from ref 52. Copyright 2006 Royal Society of Chemistry.

and anisotropy. Various methods implying the reduction of metal salts, oxides, or metal complexes either in the gas phase, or by wet chemical and electrochemical methods have been described in the literature.^{3,16,17} In the last eight years, the chemical reduction of a metal salt in solution in the presence of a soft templating or capping agent appeared to be a very successful approach for producing well-faceted metal NCs with well-controlled shapes and sizes. Works have been done using surfactant templates as nanoreactors for the growth of Cu nanorods in inverse micelles of AOT, for example,^{5,18} and of gold nanorods in alkyltrimethylammonium bromide.¹⁹ In most cases, templating agents and stabilizing agents used to protect particles from aggregation are reported to be able to adsorb selectively onto a specific crystallographic facet^{20,21} A kinetic control of the growth is reported to be achieved along one or two specific axes depending on surface energies ratio between the different crystal facets. The adsorption agent may be a molecular ligand, such as phosphine or amine.²² The use of a polymer like PVP was also very successful and extensively studied via polyols methods,^{23–27} or surfactants, such as CTAB and SDS.^{28–30}

Among these methods, some authors considered another way to improve the growth control of particles and consequently their morphology: the use of beforehand prepared seeds. The seed-mediated methods were first employed to

control the particle size, and then developed to obtain various nanostructures.^{27,31–34} They are based on the decoupling of nucleation and growth kinetics. This principle is currently used in polyol methods, but also in aqueous synthesis in the presence of a surfactant. The most famous seed-mediated synthesis using CTAB as a selective adsorption agent is reported for gold NCs exhibiting specific morphologies.³¹ Either mix or single morphologies (rods, cubes, tetrahedra, spheres, etc.) have been obtained (cf. Figure 1).⁵² Numerous parameters seem to play a critical role in the formation of these particles. In particular, studies have been focused on the role of the surfactant³⁶ as well as on the influence of size, structure, and nature of seeds.³⁷ Although presented as “simple” kinetically controlled synthesis, the exact role played by each component of the synthesis onto the final mix of morphologies, shapes, and sizes (surfactant, reducing agent, seed size and shape, temperature, solvent, surface energy stabilization of the different crystallographic facets of the growing NCs, etc.) is only partially understood. More specifically, the influence of the seed crystallographic structure (monocrystalline or twinned seeds) has not been thoroughly addressed, mainly because of the difficult characterization of the crystalline structures of very small objects (a few nanometers usually). It is still not clear whether the twinned NCs obtained, called “multiply-twinned particles” (MTP) (mainly pentwinned decahedra and nanorods) take their origin from the crystalline structure of the seed or are promoted by an aggregative mechanism taking place when seeds are mixed with metallic salt of the growing solution.³⁸ Nowadays, mechanisms based on conventional nucleation process and controlled aggregation yielding to mesocrystals are the matter of many lively scientific debates.^{10,38–41}

- (16) Yagi, K.; Takayanagi, K.; Kobayashi, K.; Honjo, G. *J. Cryst. Growth* **1975**, *28*, 117–124.
 (17) El-Deab, M. S.; Sotomura, T.; Ohsaka, T. *J. Electrochem. Soc.* **2005**, *152*(11), C730–C737.
 (18) Pileni, M. P. *C. R. Chim.* **2003**, *6*(8–10), 965.
 (19) Nikoobakht, B.; Wang, Z. L.; El-Sayed, M. A. *J. Phys. Chem. B* **2000**, *104*(36), 8635.
 (20) Puntès, V. F.; Krishnan, K. M.; Alivisatos, A. P. *Science* **2001**, *291*(5511), 2115.
 (21) Gregorio, D.; Bisson, L. *Appl. Catal., A* **2009**, *352*, 50.
 (22) Philippot, K.; Chaudret, B. *C. R. Chim.* **2003**, *6*(8–10), 1019.
 (23) Chen, J.; Herricks, T.; Geissler, M.; Xia, Y. *J. Am. Chem. Soc.* **2004**, *126*(35), 10854.
 (24) Kim, F.; Connor, S.; Song, H.; Kuykendall, T.; TYang, P. *Angew. Chem., Int. Ed.* **2004**, *43*(28), 3673.
 (25) Sun, Y.; Xia, Y. *Adv. Mater.* **2002**, *14*(11), 833.
 (26) Giersig, M.; Pastoriza-Santos, I.; Liz-Marzan, L. M. *J. Mater. Chem.* **2004**, *14*, 607–610.
 (27) Zou, K.; Zhang, H. X.; Duan, X. F.; Meng, X. M.; Wu, S. K. *J. Cryst. Growth* **2004**, *273*, 285–291.
 (28) Chen, S.; Carroll, D. L. *J. Phys. Chem. B* **2004**, *108*(5), 5500.
 (29) Kuo, C. H.; M.H., H. *Langmuir* **2005**, *21*(5), 2012.
 (30) Lim, B.; Jiang, M.; Tao, J.; Camargo, P. H. C.; Zhu, Y.; Xia, Y. *Adv. Funct. Mater.* **2009**, *19*, 189–200.
 (31) Jana, N. R.; Gearheart, L.; Murphy, J. C. *J. Phys. Chem. B* **2001**, *105*, 4065–4067.
 (32) Chen, C.; Wang, L.; Jiang, G.; Yang, Q.; Wang, J.; Yu, H.; Chen, T.; Wang, C.; Chen, X. *Nanotechnology* **2006**, *17*, 466–474.

- (33) Berhault, G.; Bisson, L.; Thomazeau, C.; Verdon, C.; Uzio, D. *Appl. Catal., A* **2007**, *327*, 32–43.
 (34) Grzelczak, M.; Pérez-Juste, J.; Mulvaney, P.; Liz-Marzan, L. M. *Chem. Soc. Rev.* **2008**, *37*, 1783–1791.
 (35) Sau, T. K.; Murphy, J. C. *J. Am. Chem. Soc.* **2004**, *126*, 8648–8649.
 (36) Gao, J.; Bender, C. M.; Murphy, J. C. *Langmuir* **2003**, *19*, 9065–9070.
 (37) Gole, A.; Murphy, J. C. *Chem. Mater.* **2004**, *16*, 3633–3640.
 (38) Stoeva, S. I.; Zaikovski, V.; Prasad, B. L. V.; Stoimenov, P. K.; Sorensen, C. M.; Klabunde, K. J. *Langmuir* **2005**, *21*, 10280–10283.
 (39) Cölfen, H.; Antonietti, M. *Angew. Chem., Int. Ed.* **2005**, *44*, 5576–5591.
 (40) Niederberger, M.; Coelfen, H. *Phys. Chem. Chem. Phys.* **2006**, *8*, 3271–3287.
 (41) Jonhson, C. J.; Dujardin, E.; Davis, S. A.; Murphy, J. C.; Mann, S. *J. Mater. Chem.* **2002**, *12*, 1765–1770.

Of course, in some other methods used to prepare anisotropic NCs, the growth mechanism is better understood. For example, in template methods, metallic NCs are often formed by uncontrolled aggregation of primary particles.²⁷ But this type of mechanism leads mainly to polycrystalline nanoparticles (NPs), which limits their interest for any application demanding well-faceted NCs such as selective catalysis. More recently, a general crystal formation mechanism, made of epitaxially aggregated nanoparticles, emerged in the literature for explaining the existence of some macrocrystalline superstructures called mesocrystals. Specific investigations on many systems (metal carbonates, sulfates, or oxides) permitted us to observe that an oriented attachment of preformed nanocrystals could be triggered by a careful tuning of NC surface energy, leading to a global self-assembly of primary particles, coordinated with each other by similar crystallographic facets.^{1,26,39,42–44} In this case, the assembly of nanobuilding blocks usually leads first to mesocrystals and eventually to the formation of one-piece monocrystals. Descriptions of those systems are more complex but in many cases much more realistic than “classical crystallization” events, covered by classical nucleation and growth theories, which describe growth by molecule or ion-by-ion attachment. As far as we know, only one study has been dedicated to synthesis of metallic single nanocrystals presenting specific morphology obtained by a random aggregative mechanism. In a synthesis by solvent reduction in *N,N*-dimethylformamide (in presence of poly(vinylpyrrolidone)), a HRTEM demonstration of the aggregation of Ag precursor NCs through preferred facets leading to monocrystalline nanowires has been given by Giersig et al. in 2004.²⁶

In the present paper, we studied the extension of the seeding-mediated synthesis of gold NCs in an aqueous medium in the presence of CTAB described by Murphy's group³¹ to the case of palladium. In a first preliminary study, Berhaut et al.³³ proved that a similar experimental protocol leads to the formation of a wide variety of NCs with morphologies similar to those formed with gold metal (described in figure 1). However, in the present work, the detailed study of the evolution of palladium NCs sizes and shapes as function of time gave results disagreeing with the kinetically controlled differentiation of shapes mechanism reported for gold NCs. On the opposite of the gold synthesis, the systematic presence of numerous very small palladium spherical nanoparticles (nuclei) generated by homogeneous nucleation within the solution after seeds introduction was noted. By very carefully investigating the different steps of NCs formation, we observed an early aggregation of seeds and nuclei leading to the formation of secondary objects of nonrandom shapes, the growth of which led to the final well-faceted palladium NCs. Usually, works found in the literature determine what is the specific set of experimental conditions needed to obtain a specific NP shape. Consequently, it is

sometimes difficult to strictly determine the influence of each parameter on one specific shape of NPs at similar synthesis condition. In this work, we adopted a different approach consisting in observing a solution containing a mix of NPs shapes on which we studied the influence of a determined variation of experimental parameter. This original approach allowed us to compare, at similar experimental parameters, the size evolution of each shape and the influence of secondary nucleation phenomenon on NPs generation and growth. With a systematic investigation of the synthesis parameters, we could identify the most probable formation mechanism. Differently from previously reported mechanisms, an oriented attachment of seeds and nuclei triggered by the energetically most favorable stacking of spheres was found to be responsible for the early differentiation of the NC shapes. The original formation mechanism presented here is strongly supported by experimental facts. It shed a new light on the seed-mediated synthesis of palladium NCs by (i) explaining the shape differentiation via an oriented attachment process and (ii) explaining in detail the influence of CTAB surfactant, seeds size on nuclei size ratio, solvent, and temperature onto the final NCs shapes. In addition, it allows the unprecedented rationalization and the prediction of the aspect ratio variation of the pentatwinned nanorods diameter as a function of the seed on nuclei diameter ratio.

Experimental Section

Materials. Potassium tetrachloropalladate (K₂PdCl₄, 98%), cetyltrimethylammonium bromide (CTAB), sodium borohydride (NaBH₄, 98%), and sodium L-ascorbate (98%) were purchased from Sigma Aldrich. All aqueous solutions of potassium tetrachloropalladate, cetyltrimethylammonium bromide, sodium borohydride, and sodium L-ascorbate (98%) were freshly prepared before use.

Synthesis of Pd Seeds and Nanostructures in Aqueous Medium. Typically, a seed solution containing Pd small nanoparticles was prepared by adding at 30 °C 12.5 mL of a 1 mM K₂PdCl₄ solution with 25 mL of 0.15 M CTAB solution. Then, 3 mL of an ice-cold 0.01 M NaBH₄ solution was quickly added under vigorous stirring. The solution turned brown immediately after the borohydride addition, indicating metallic palladium nanoparticles formation. The palladium suspension was stirred for 15 min. The seed solution was used systematically 2 h after its preparation. This period of time is necessary for complete decomposition of excess NaBH₄. The growth solution was obtained by mixing at 30 °C 25 mL of a 3 mM K₂PdCl₄ solution with 25 mL of a 0.24 M CTAB solution under gentle stirring. After 5 min of mixing, the solution turned deep orange and an orange turbid suspension formed. The precursor present in solution was characterized by UV-visible spectroscopy to be [PdBr₄]²⁻ resulting from ligand exchanged of [PdCl₄]²⁻ by bromide from the CTAB. The suspension is made of micrometric platelike crystals of composition PdBr₄(C₁₆TA)₂.³³ One mL of a 0.08 M sodium ascorbate solution was then added. Finally, palladium nanostructures were formed by injecting 90 μL of the seed solution into this growth solution. The initial orange red solution changed progressively in 30 min into a dark solution indicating the reduction of the metallic precursor. The initial turbidity progressively disappeared with the progressive reduction of Pd (II).

(42) Judat, B.; Kind, M. *J. Colloids Interface Sci.* **2004**, *269*(2), 341–353.

(43) Tang, Z. Y.; Kotov, N. A.; Giersig, M. *Science* **2002**, *297*(5579), 237–240.

(44) Krishnaswamy, R.; Remita, H.; Imperor-clerc, E., C.; Davidson, P.; Pansu, B. *Chem. Phys. Chem* **2006**, *7*(7), 1510–1513.

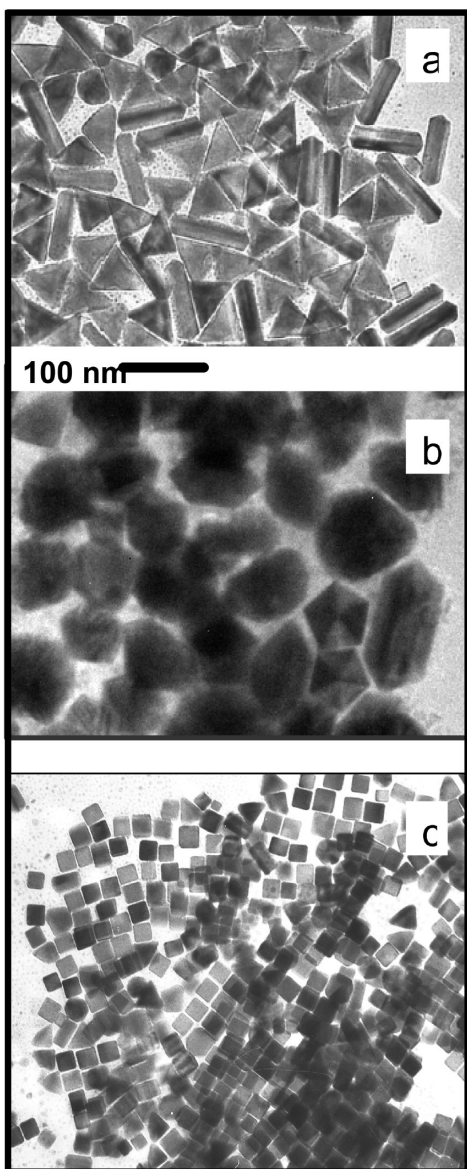


Figure 2. TEM picture of Pd NCs prepared (a) with and (b) without seeds at 30 °C and (c) without seeds at 65 °C.

Synthesis of Gold Nanostructures in Aqueous Medium. Gold NCs synthesis was reproduced from a Sau et al. work.³⁵

Characterizations. Time resolved Transmission electron microscopy studies were performed in a JEOL 100CX2 (W filament) and in a Philips TECNAI F20, both operating at 200 kV. TEM images were digitally recorded by a CCD camera. TEM grids (300 mesh copper grids) preparation mode was revealed to be of paramount importance for reproducibility of analysis. An efficient quenching of the nanostructure evolution onto the grid at a given reaction time was obtained by placing the copper grid directly onto a filter paper before deposition in order to instantaneously suck the excess solution out of the grid. This prevents any evolution of the deposited particles during their drying time. Deposited grids were then rinsed several times with cold ethanol drops to remove the surfactant. Particle size distributions and corresponding statistical analysis of the different morphological types of nanoparticles were obtained from TEM images by using analySIS software. In each case, at least 200 particles were counted. The as-synthesized Pd growth solutions maintained at 30 °C were analyzed by UV-vis/near IR spectroscopy using a Uvikon XL (Secoman) spectrophotometer in the 200–800 nm

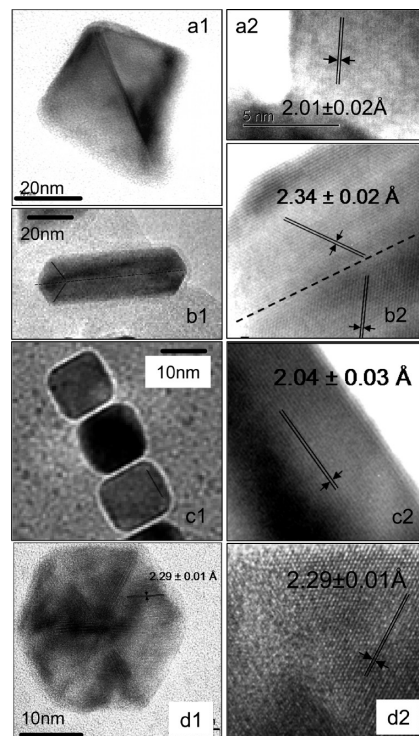


Figure 3. HR-TEM pictures of Pd NPs of different shapes prepared with seeds obtained after 3 h of reduction: (a) pyramid, (b) pentatwinned nanorods, (c) cube, and (d) icosahedra.

wavelength range. The UV-vis analyses were performed with cells of 2 and 5 mm thickness. In Figure 4, the absorbance was normalized to an optical length of 1 mm.

Results

Palladium nanocrystals (NCs) exhibiting well-defined morphologies can be obtained by a seed-mediated aqueous synthesis in the presence of CTAB surfactant. The preparation of these metallic particles implies two steps. At first, few nanometer Pd seeds are prepared via the fast chemical reduction of a palladium salt by sodium borohydride in the presence of CTAB as a stabilizing agent.³³ In the second step, a small amount of a 2 h old seed solution is quickly mixed with a growth solution containing palladium salt, CTAB and ascorbate as weak reducing agent. Pd⁰ NCs exhibiting well-defined morphologies are then formed (Figure 2a). According to time-resolved UV-vis (Figure 4), we could determine that the reduction of palladium salt was almost completed after 3 h.

A standard TEM observation of these solutions after 3 h showed (Figure 2a) five distinct geometries of NP obtained from HRTEM: rods of 5-fold twinned symmetry with five long lateral (100) faces and ten tip (111) faces (Figure 3b1 and b2), triangular pyramid-shaped nanoobjects exhibiting three (100) and one (111) faces (Figure 3a1 and a2), a few hexagonal-shaped nanoobjects attributed to icosahedra (Figure 3d1 and d2), cubes with six (100) faces (Figure 3c1 and c2), and a few isotropic crystalline particles of size smaller than palladium seeds introduced for the reaction. Structures of these particles were described elsewhere.³³ Interreticular distances

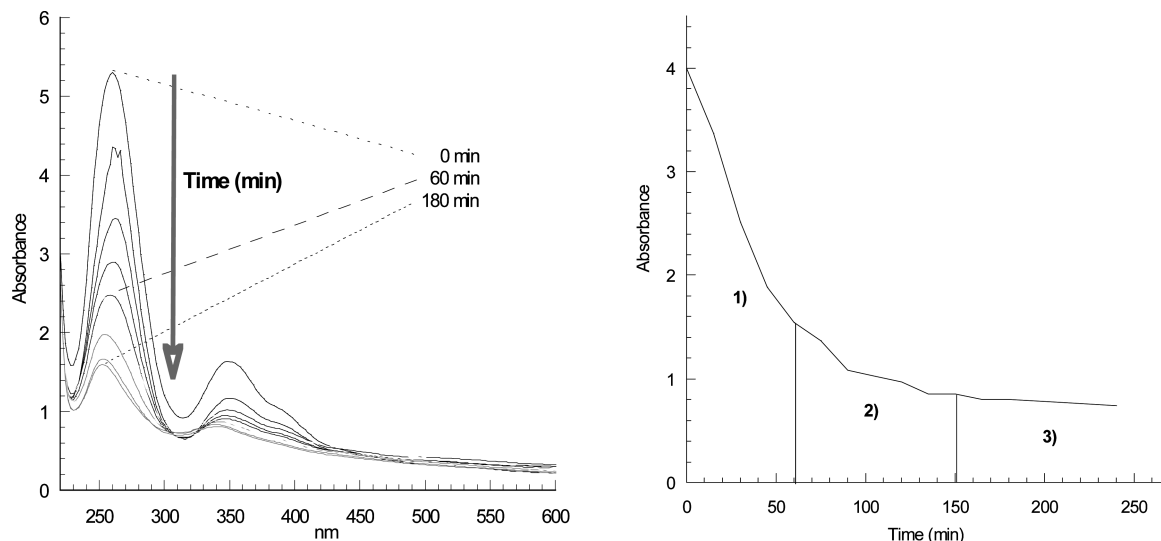


Figure 4. (Left) UV-vis spectra of the solution as a function of reaction time after seeds introduction. (Right) Plot of the absorbance of $[\text{PdBr}_4]^{2-}$ at 255 nm.

measured by HRTEM – 2.29 or 2.34 Å for (111), and 2.01 or 2.04 Å for (200) plans – are slightly larger than expected for pure Pd crystals. They are either due to crystalline structure deformation sometimes observed with NPs or due to the presence of hydrides into the crystalline framework, known for being stable at ambient temperature and dilatating the crystalline framework of Pd. According to literature, the resulting formula of such hydride palladium NCs could correspond to PdH_x with x value equal to 0.67.⁴⁵

Two reference reactions were performed without seeds addition at 30 and 65 °C. The 30 °C reaction without seeds produced much bigger Pd^0 NCs (about 100 nm), some being well-faceted and the others exhibiting poorly defined shapes, as can be seen in Figure 2b. In this case, almost no rodlike or pyramidal NPs were observed. Instead, ill-defined multiply twinned decahedral particles (MTDP) with ten (111) faces were observed. This type of NCs was previously described in the literature as being at the origin of nanorods.^{41,46} At 65 °C without seeds, the reaction produced in very high yield cubic palladium NCs of 15 nm exhibiting (100) oriented facets. These cubic NCs are very similar to those prepared by Sun et al. in the presence of citric acid with ascorbic acid as reducing agent.⁴⁷ Yet, in our case, no mix of cubes and rectangular particles was observed, probably because no citrate was used.

From these simple reference experiments come several observations. First, a homogeneous nucleation of Pd^0 NPs can take place spontaneously in a CTAB rich solution of palladium salt and ascorbate. Second, the rate of this homogeneous nucleation is of major importance for controlling the final shapes of NCs. At low temperature, a slow nucleation rate (vide infra) promotes the coexistence

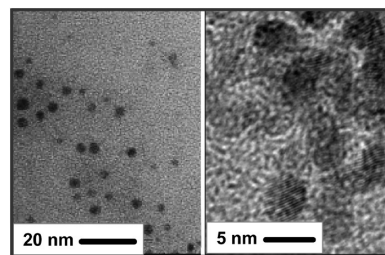


Figure 5. HRTEM pictures of NPs from the 2 h old seed solution.

of small (young) nuclei and big (older) nuclei, leading to the formation of various types of NCs. At high temperature, a fast nucleation rate leads to a homogeneous growth of cubes. As a consequence, it seems (i) that the existence of a distribution of colloid size in solution (either by slow homogeneous nucleation or seed addition) within the growing solution promotes the formation of several NC morphologies; (ii) that the presence of already made seeds (leading to a bimodal particle size distribution) is mandatory for the production of pyramids and anisotropic Pd^0 pentatwinned nanorods.

Kinetic Study. To understand why the presence of seeds promotes NC shape changes and the appearance of a significant proportion of anisotropic objects, we carefully investigated particles morphologies evolutions by TEM and HRTEM in the early stages of the reaction. Samples were taken out of the reaction mixture every 3 min of the first 30 min and quickly deposited onto microscopy grids prepared according to the fast draining process described in experimental section.

Two hours old particles used for seeding were spherical single crystals of 5.6 ± 1.2 nm (Figure 5). One minute after the introduction of seeds in the growth solution, two distinct populations of particles were observed (Figure 6). One was attributed to the seeds growing by molecular reduction (their mean size, 7–8 nm, is slightly bigger than their original size). The other NPs of average diameter 2–3 nm, were assumed to be the nuclei resulting from the homogeneous nucleation process occurring when

- (45) Muetterties, E. L. *Transition Metal Hydrides*; Marcel Dekker: New York, 1971; Vol. 11
 (46) Perez-Juste, J.; Liz-Marzan, L. M.; Carnie, S.; Chan, D. Y. C.; Murvaney, P. *Adv. Funct. Mater.* **2004**, *14*(6), 571–579.
 (47) Sun, Y.; Zhang, L.; Zhou, H.; Zhu, Y.; Sutter, E.; Ji, Y.; Rafailovich, M. H.; Sokolov, J. C. *Chem. Mater.* **2007**, *19*, 2065–2070.

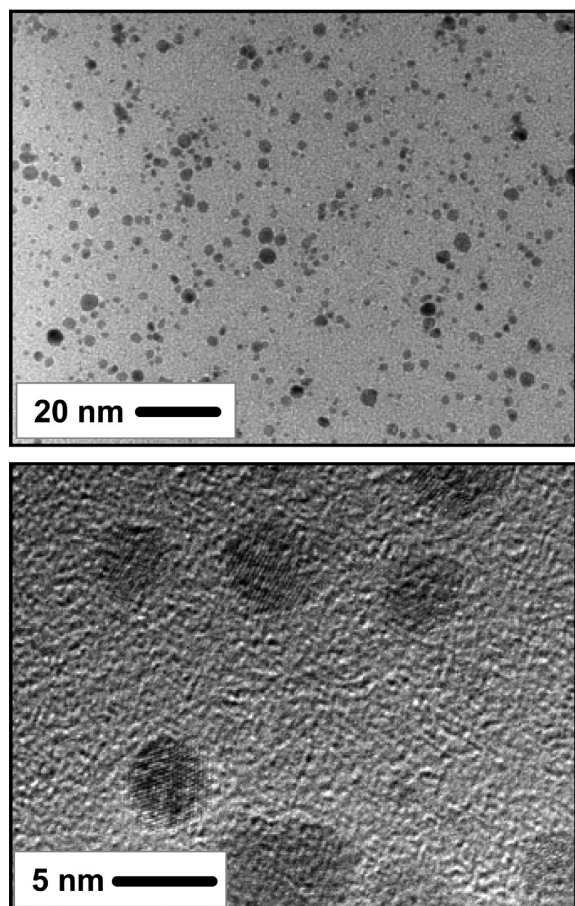


Figure 6. TEM pictures of NPs from the reactive solution taken 1 min after the introduction of seeds.

ascorbate is introduced in the growth solution. These latter particles were shown to be spherical and, from HRTEM, monocrystalline. After 3–6 min of reaction, the above-described seeds and nuclei tended to aggregate, leading to the formation of secondary particles. In Figure 7, TEM images at this stage showed that big and small particles are packed together in a determined way, forming the first drafts of triangular, cubic, or rodlike shapes of the final NCs. A closer observation of aggregates showed that seeds and nuclei often maintain an intermediate distance which value is regular and very close to the thickness of a bilayer of CTAB molecules (see the Supporting Information, S11). Hence an intermediate step of secondary particles formation is very likely an adsorption of nuclei on seeds (or nuclei on nuclei) via the sharing of a CTAB bilayer as schemed hereafter. At the same time, nuclei coalescence could be seen at the surface of secondary particles (images b and c in Figure 7), indicating that palladium could diffuse from the solution to the metallic surface, probably via the adsorbed CTAB bilayer as described by Nikoobakht et al.⁴⁸ Thus, the simultaneous seed–nuclei aggregations and molecular reduction led to secondary particles consisting of already differentiated and oriented nanocrystallites with grain boundaries. The FT analysis of TEM pictures of these particles (one example is given in

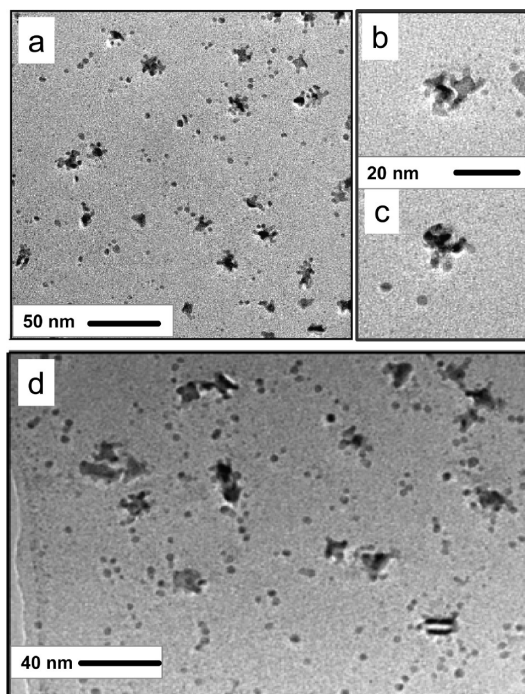


Figure 7. TEM pictures of NPs from the reactive solution taken (a–c) 3 and (d) 6 min after the introduction of seeds.

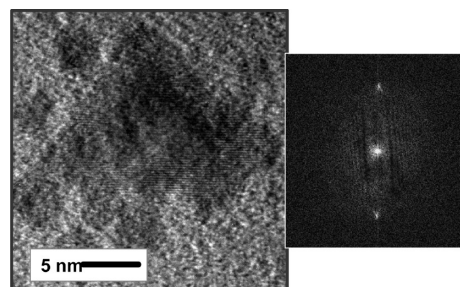


Figure 8. TEM pictures of one NCs from the reactive solution taken 6 min after the introduction of seeds (left) showing the structuration of a pyramidal particle and (right) its Fourier transformation.

Figure 8) clearly shows that although irregularly packed at this time, all seed and nuclei of a secondary particle present crystallographic mono-orientation. After 9 min, the before schemed morphologies of Pd secondary particles are clearly defined with core structures either monocrystalline or twinned, as can be seen by the presence of “moirés” on nanorods and pyramids (Figure 9). Thus, grain boundaries and cavities between nuclei must have disappeared during the aggregation–reduction processes. As we will show, at this stage, NCs are growing very fast, and because of nuclei aggregation, their surfaces are rough. Cubic NCs seems to incorporate nuclei preferentially by corners when pyramid NCs do it by the edges and rod NCs do it by the tips. Up to 20 minute of reaction, we always observed the presence of small nuclei concomitantly with the structured NCs. During this period, UV–vis monitoring attested that the $[\text{PdBr}_4]^{2-}$ concentration is maintained at a high level because of the progressive dissolution of the $\text{PdBr}_4(\text{CTA})_2$ suspension acting as a palladium salt reservoir. We assumed that salt saturation level was kept high enough to generate

(48) Nikoobakht, B.; El-Sayed, M. A. *Langmuir* **2001**, *17*, 6368–6374.

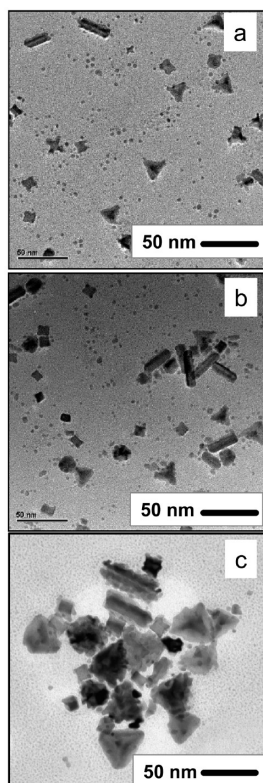


Figure 9. TEM pictures of NCs from the reactive solution taken (a) 9, (b) 12, and (c) 20 min after the introduction of seeds.

constant secondary nucleation, thus maintaining a constant supply of nuclei in the reaction mixture, providing matter for particles formation and growth. Thereafter, between 15 min and 4 h, particles grew uniformly, and simultaneously, their facets were smoothed. During this period of time, the Pd bromide precursor was still being chemically reduced as observed by spectroscopy UV–visible (cf. Figure 4), although the number of nuclei observed decreased significantly after 15 min.

The morphological evolution of NCs with time was reported in Figure 10. One noticed as a general trend that NC growth seems to happen in two steps, a first explosive growth in the early 15 min followed by a slower and progressive evolution. Rod length and diameter, reported in Figure 10a, evolved differently. The increase in rod diameter stopped after 40 min, when rods length was still increasing after 3 h. As a consequence, the resulting rods aspect ratio was continuously increasing with time, attesting that the matter incorporated preferentially by the ends (or tips) of the rods in the first fifteen minutes and almost only by the ends after 40 min. Cubes, pyramids, icosahedra, and nuclei NC size evolutions are reported in Figure 10b. For these particles, we also noticed an explosive growth, followed by a slower growth. Yet, in this case, final particles sizes were fixed after only 40–50 min of reaction. After this delay, rods were the only particles still growing in the solution.

The formation of palladium NCs by this seed-mediated synthesis thus results from two combined growth mechanisms: (i) at short reaction time, a fast aggregation of seed and nuclei leading to the formation of secondary particles

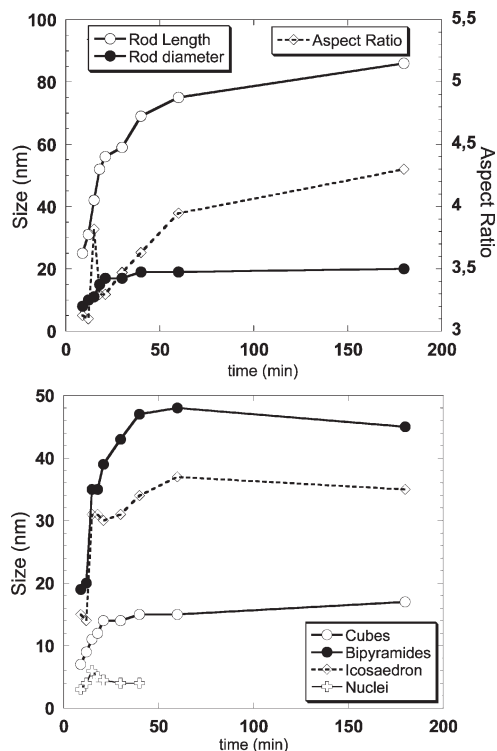


Figure 10. Final NPs size evolution as a function of reduction time for (a) nanorod length, diameter, and aspect ratio, (b) from bottom to top, nuclei, cubes, icosahedra, and pyramids.

with crystalline mono-orientation, concomitant with molecular reduction; (ii) at long reaction time, a conventional molecular reduction of the palladium bromide.

Seed Size Influence. The reference syntheses performed without seeds have proven that seeds are essential for obtaining shape-controlled particles, and in particular, rods and pyramidal Pd NCs. To determine the influence of the seeding onto the final NCs geometries, identical experiments with seeds of various sizes (obtained by using older seed solutions) were performed. The same volume of seeding solution was used for each experiment. Final morphologies evolutions (determined for 48 h old structured NCs) are reported in the figure 11 for pyramidal, icosahedral, cubic, and five-twinned rod NCs. By varying seeds size from 3.9 to 11 nm, three distinct behaviors were observed.

The obtained pyramidal and icosahedral NCs were significantly bigger when bigger seeds were used. This suggests that seeds introduced are involved in the formation of pyramids and icosahedra shaped NPs. Yet, the size gain (about 22 nm) is larger than the seed size increase (7 nm). This difference is likely to be due to the fact that the same weight of Pd⁰ was introduced in each seeding. Bigger seeds are less numerous. Hence, the continuous growing of NCs is both due to bigger seeds and to lower seeding rate.

The increase in seed diameter did not influence cube size very much. Starting from the reference synthesis performed at 65 °C, which exclusively produced nanocubes, we assumed that cubic NCs observed when seeds are used are the result of the aggregation and/or growth of nuclei only. The small increase in cube size observed for

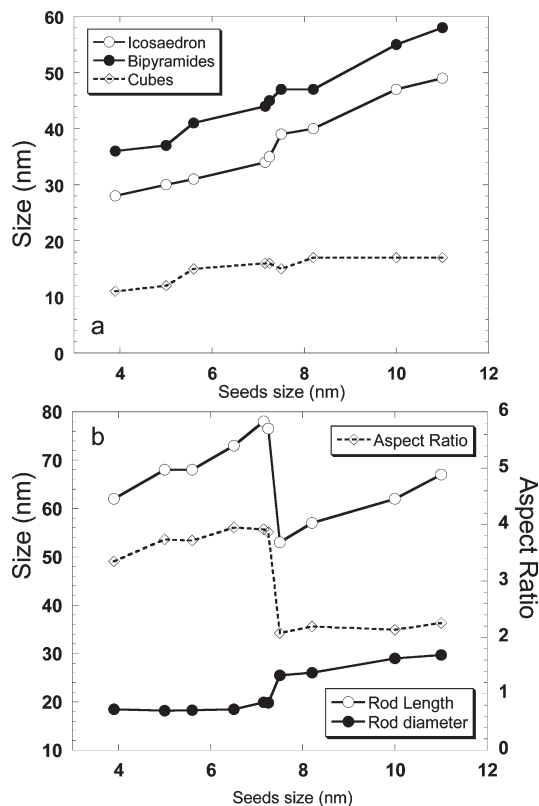


Figure 11. Final NP size evolution as a function of the seed diameter.

small seeds (4–7 nm, see Figure 11) was probably due to a variation in the relative number of cubes formed and, hence, to the relative proportion of palladium incorporated during their molecular growth.

Rod length, diameter, and aspect ratio were almost constant for seed diameter < 7 nm. Then, a sudden shape change occurred when using seeds of size 7–7.5 nm. All nanorods are then much shorter and wider, corresponding to an aspect ratio decrease of nearly 40%. It is noteworthy that further increasing seed size from 7.5 to 11 nm (that is 3.5 nm more) promoted almost no rod diameter increase (3.5 nm) but a significant rods length increase of 14 nm. In the same way than for pyramids and icosahedra NCs, 5-fold nanorods dimensions are very dependent on the seed size. Hence, we assumed that they are the result of the aggregation and growth of (at least) one seed and several nuclei.

A last experiment consisted in the functionalization of seeds surface using tri sodium citrate as a stabilizing agent in place of CTAB in the seeding step. The seeds obtained were less homogeneous in size (2–7 nm) and morphology. Particles formed using these modified seeds were poorly structured polyhedra of diameter 60–75 nm, with some cubes (7–10 nm). One assumed that the adsorption of citrate at the surface of the seeds disturbed the very first minutes of the aggregation–reduction reaction where the organized aggregation occurs. This disturbance came probably from an adsorption competition between the CTAB of the growing solution and the preadsorbed citrate. The formation of CTAB bilayer at the surface of the seeds is then hindered for a time, making difficult

the sharing of a CTAB bilayer between seeds and nuclei. This experiment stresses the critical influence of the very first minutes of the aggregation process and explains why in this case the obtained NCs were very similar to those obtained in a synthesis performed without seeds.

Discussion

The homogeneous nucleation of spherical nuclei and their self-assembly is clearly confirmed by TEM observations, but the appearance of these specific and eventually regular structures is not so easy to rationalize via purely aggregative mechanisms. The early aggregation of seed and nuclei creates intermediate secondary particles with morphologies similar to those of intermediate particles observed in mesocrystals formation. Both are imperfectly ordered aggregates with epitaxial crystalline orientation.³⁹ Yet, instead of a single type of mesostructure (usually reported for mesocrystals), the oriented aggregation of seeds and nuclei produces NCs of different symmetries and structures, some with and some without twin planes. In the early stage of the reaction, these polycrystal intermediates conserve their symmetry axis while growing continuously, both by aggregation of other nuclei and molecular reduction. After 12 min of reaction, the number of nuclei decreases dramatically, allowing molecular surface reduction to be the dominant growth process. Obviously in the Pd case, the convincing formation mechanism proposed for the structuration of gold NCs prepared in similar conditions (that is a seeding followed by the CTAB-assisted control of seeds growth by molecular surface reduction with conservation of both the crystalline structure and the symmetry of the seeds), is not valid anymore. In this section, we proposed a credible formation mechanism taking into account the role of critical parameters such as the need of CTAB surfactant and seeds for obtaining anisotropic NCs. This mechanism explains satisfactorily (i) why in the early stage of the reaction, seeds and nuclei attach with each other in an oriented way, (ii) the influence of the seed size onto final NCs' morphologies. Very interestingly, this mechanism proposes a way to rationalize and predict the abnormal steplike variation of nanorods diameter when seeds diameter changes.

Step 1: Oriented Attachment. As evidenced by the time-resolved TEM study, just after seeds addition, two populations of nanoparticles are cohabiting, seeds of 5–6 nm and nuclei of 2–3 nm coming from homogeneous nucleation of the solution. Attending the high CTAB concentration of the solution, all of them are doubtlessly covered by a surfactant bilayer that maintains them in solution and slows down their growth.⁴⁸ A strong attractive interaction is assumed between the palladium surfaces and the CTAB. As shown schematically in panels a and b in Figure 12, when two particles collide in such a medium, they first adsorb on each other by sharing the same surfactant bilayer. This bilayer is literally a supported liquid layer that allows the rotation on itself and the circulation on each other of each adsorbed colloid.

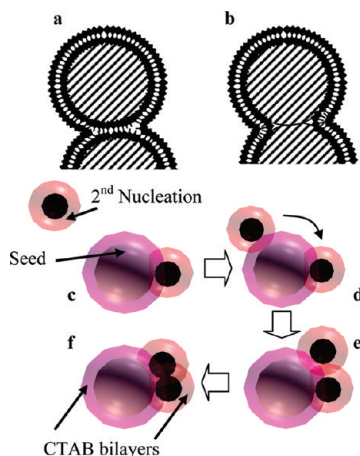


Figure 12. Scheme of the seed-nuclei oriented attachment process. (a) Adsorption of two colloids by sharing of a CTAB bilayer, (b) resorption of the shared CTAB and locking of the aggregation with epitaxial matching. (c, d) Adsorption and 2D-diffusion of a nucleus onto seed surface, (e) locking of the adsorption by double sharing of CTAB bilayer, (f) aggregation and locking of the aggregation with epitaxial matching.

Although, in such a configuration, some CTAB packing faults (forming a triple point corona) exist at the interface of the colloids, acting like bilayer edge with surfactant packing faults. The adsorption of colloids is thus very probably metastable and the system evolves spontaneously in order to minimize its free enthalpy, either by desorbing colloids or by resorbing the edge defaults (Figure 12b). This free enthalpy minimization corresponds to the stabilization of a model surfactant bilayer of finite size that spontaneously stabilizes by merging with other bilayers (thus eliminating edges).⁴⁹ The consequence of the edge resorption is the aggregation of the colloids that are then quickly locked by the continuous reduction of palladium salt at the surface of NPs. At this step, the stronger is the adsorption of CTAB onto a specific Pd crystalline surface, the more difficult it is to remove it from this surface.

In a similar way, when a nucleus adsorbs and diffuses at the surface of a secondary particle built by “1 seed–1 nucleus” aggregation (panels c and d in Figure 12), it is preferentially stabilized at the “seed–nucleus” junction by sharing more of its bilayer (Figure 12e). The resorption of the defaults leads to a “1 seed–2 nuclei” particle. By adding more nuclei, one sees that the geometry of the aggregates is obviously not random but oriented by the presence of preferential adsorption sites at the junction of two, three, or four other colloids. The more stabilizing is the adsorption site, the faster the adsorption and aggregation on this site will be. As consequences: (i) The size of the particles, therefore the curvature of their supported CTAB bilayer, modifies their free enthalpy of adsorption. (ii) If little stabilization difference exists between two types of stabilization sites, a differentiation of secondary objects is likely to occur and several secondary particles packing geometries are obtained. Thus, one understands the high versatility of this system to any parameter able to

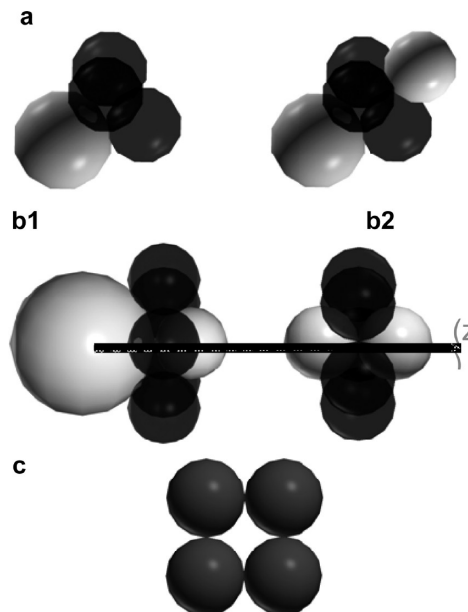


Figure 13. Schemes of spheres stacking corresponding to the secondary particles at the origin of (a) pyramids and twinned pyramids, (b1) pentatwinned nanorods, (b2) pentatwinned decahedron, and (c) cubes NCs.

alter the CTAB bilayer integrity (e.g., lower CTAB concentration, cosurfactant or cosolvent adjunction, ionic strength) or the CTAB adsorption energy during the seed–nuclei aggregation period (presence of a chemical species such as citrate competing with CTAB for adsorption, for example). (iii) The surface of colloids being charged by the CTAB bilayer, an approaching nucleus suffers less electrostatic repulsion from the more curved surfaces. Hence, additional nuclei may aggregate preferentially onto the edges and tips of secondary particles, promoting local anisotropy.⁴⁶

From this secondary particle generation mechanism, we drew the most probable first step of the palladium NCs generation. For a very large majority, NCs produced here by this seed-mediated synthesis are pyramids or twinned pyramids, small cubes, and pentatwinned nanorods. As seen in the experimental section, cubes are likely to form by the aggregation of nuclei only (Figure 13c). Pyramids are probably resulting from secondary particle made by the oriented attachment of one seed and three or four nuclei (Figure 13a).

The explanation of the formation of the pentatwinned NCs (that is decahedra formed in the reaction without seeds, and the pentatwinned nanorods formed in the reaction with seeds) is more complex attending that both the pentatwinning and the symmetry five axis formations have to be addressed. As no twinned seed has been observed on HRTEM study, the most realistic assumption is that twinning is resulting from an aggregation process, as observed for the formation of metallic NPs in vacuum deposition experiments.¹⁶ Such an aggregation must imply one seed (or one nuclei for the synthesis without seeds) and some nuclei. Yet, by respecting the aggregation rules given here above, there is only one way of creating a very stable secondary particle with

(49) Israelachvili, J. N.; Mitchell, D. J.; Ninham, B. W. *J. Chem. Soc., Faraday Trans.* **1976**, *11*(72), 1525.

a symmetry five axis. Indeed, when successive nuclei adsorb onto a “1 seed–1 nucleus” group, they stabilize better at the seed–nucleus junction and form a necklace (Figure 13b) of five nuclei. This is a very stable seven-particle configuration, often found in clusters and latex-bead-controlled aggregation preparation, which forms easily because it corresponds to a minimum second moment of mass distribution.⁵⁰ At this stage, the seed-diameter on nucleus-diameter ratio is not of critical importance attending that whatever the size of the seed (even if it has the size of a nuclei), five nuclei can complete the necklace and create by this way a symmetry five axis with a high occurrence probability (see the Supporting Information, SI2). The presence of seeds in the reactive medium then produces asymmetric secondary particles (Figure 13b1), with the absence of seed promoting symmetric secondary particles (Figure 13b2), both having a symmetry five axis along a z axis.

HRTEM observations proved that the primary particles forming the secondary objects tend to reorient with each other and coalesce only when similar crystallographic facets come face to face. From a crystallographic point of view, in the presence of CTAB, the coalescence of more stable (100) facets leads to a perfect alignment of the secondary object. On the other hand, the more energetic (111) facets may lead to a secondary object twinning. Classically, literature assumes that the small spherical metallic NCs observed in the early stage of such reduction reaction are monocrystalline cuboctahedron or icosahedron, presenting mostly (111) external facets eager for stabilization.⁵¹ On gold NCs, (111) facets are likely to be less stabilized by CTAB adsorption than (100) facets.⁴¹ A similar behavior for palladium would explain that during the formation of secondary objects, aggregated nuclei stabilize better by sharing their (111) facets. Such stabilization along the symmetry five axis of b1 and b2 objects (cf. Figure 13) combined with the need of accommodating the 72° angle of the order five axis could explain the pentatwinning of (111) facets usually observed for pentatwinned nanorods and decahedra described hereabove.

Step 2: Secondary Particle Growth. According to TEM observations, secondary particles growth may be separated in two periods, (i) at short reaction time, further nuclei incorporation guided by the local energy minimizations mechanisms described here above, and concomitantly molecular reduction, (ii) after 15–20 min of reaction, by molecular reduction only, probably because palladium salt concentration falls below the homogeneous nucleation limit.

In the early stage of NCs growth, nuclei are adsorbed onto secondary objects in a nonrandom way. The aggregation rate of nuclei onto secondary particles depends

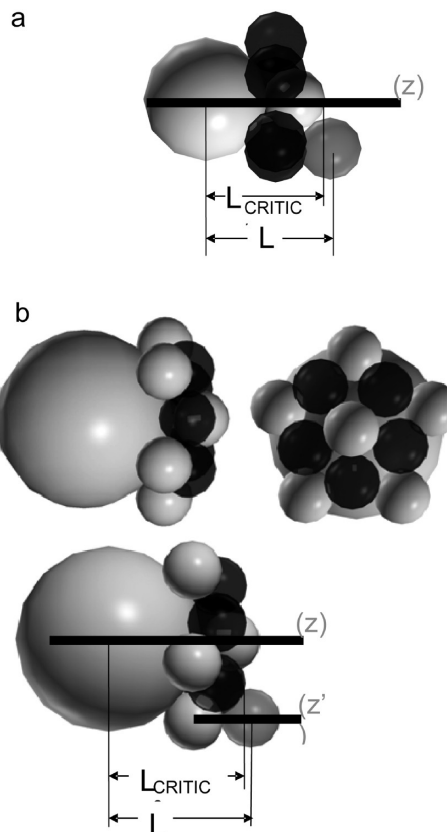


Figure 14. Scheme of spheres stacking corresponding to (a) “1 seed–6 nuclei” and, (b) “1 nucleus–11 nuclei” aggregates on which an additional nucleus adsorbs along the z axis.

on their collision frequency. According to Perez Juste et al.,⁴⁶ collisions of CTA + covered colloids are critically dependent on the electrostatic repulsions promoted by their surface potential. This repulsion decreasing with the local curvature of the CTAB bilayer, the edges and tips of the growing particles quickly becomes the sites of preferential collision if compared with the raising facets (as can be seen with early formed cubes and pyramids in Figures 7 and 8).

Pentatwinned secondary particles evolution is more complex. Indeed, the early growth is different if these secondary particles are formed from nuclei only, Figure 13b2 (pentatwinned decaedra are obtained in the seedless synthesis), or from seed and nuclei, Figure 13b1 (pentatwinned nanorods are obtained). Two hypotheses can be proposed to explain this differentiation of growth behavior. The first one, described hereabove, is that the difference in aspect ratio of the two types of aggregates could be responsible of the anisotropic growth of pentatwinned nanorods. In such a case, a preferential growth should be obtained by “preferential collision effect” along the longer axis of the secondary particle. A preferential growth along the z axis would then be possible only if the seed attains a size such as the “seed size” S_s on “nuclei size” N_s ratio exceeds 1.87. In the set of experiments described in the experimental section, the S_s/N_s ratio of seeded syntheses is always higher than 2. Thus, the experimental limit of the anisotropic differentiation of pentatwinned secondary particles could not be proved.

(50) Yang, S. M.; Kim, S. H.; Lim, J. M.; Yi, G. R. *J. Mater. Chem.* **2008**, *18*, 2177–2190.

(51) Ramos Fernandez, M. *Materials Science; Universite Pierre et Marie Curie; Paris*, 2003.

(52) Elechiguerra, J. M.; Reyza-Gasga, J.; Yamacan, M. J. *J. Mater. Chem.* **2006**, *16*, 3906–3919.

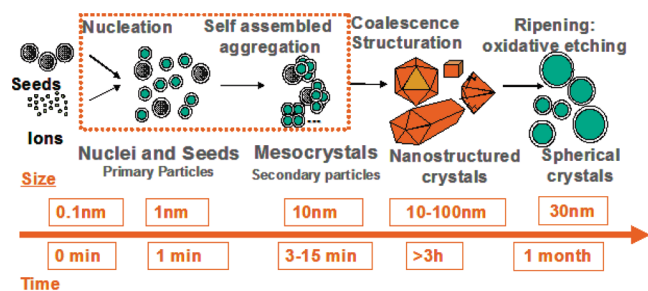


Figure 15. Summary of the nucleation and growth process for palladium nanoparticles.

The second hypothesis, based on geometric calculation, may also explain the preferential growth of nanorods along the z axis in seeded syntheses. By following the maximum stabilization rule, successive nuclei adsorb preferentially at the junction of the five nuclei corona and the axial nucleus (cf. figure 14a). It is then possible only to stack them regularly along the z direction of the considered “1 seed–6 nuclei” aggregate if the Ss/Ns ratio exceeds a certain value. If this ratio is too low (or equal to 1 for the reference synthesis in which a nucleus acts as a seed), the successive nuclei pack along directions diverging from the z axis, and quickly, no distinct preferential adsorption sites exist along the z axis anymore. As a consequence, the pentatwinned particle growth mechanism is likely to be favored via molecular reduction, and decahedra are obtained. A simple dense sphere stacking calculation, for which detail is given in the Supporting Information (see Figure 14a), shows that the axial stacking of nuclei is possible whenever $L \geq L_{\text{CRITIC1}}$, L being the height between the center of the additional nucleus and the center of the seed, along the z axis, and L_{CRITIC1} being the height between the tip of the preceding axial nucleus and the center of the seed, along the z axis. Such a calculation predicts that the axial packing is only possible if $Ss/Ns \geq 1.36$. This value is close from the experimental Ss/Ns ratio found with the “tip effect” argument. Unfortunately, the Ss/Ns critical value could not be confirmed attending that no Ss/Ns ratio lower than 2 could not be observed in our experiments. Interestingly, this model predicts that whatever the seed size bigger than the critical diameter, nanorod diameter is mainly dependent on the nuclei size; that is, the diameter of a five nuclei corona. Indeed, in our experiments, nanorod diameters have been found constant and equal to 18 nm for seeds size ranging from 4 to 7 nm. Furthermore, the above-described aggregation approach is very interesting because it allows an elegant explanation of the sudden nanorods diameter leap observed when seeds size becomes bigger than 7 nm (cf. Figure 11). Indeed, for bigger seeds, nanorod diameter suddenly leaps up by nearly 30% and remains there. This constant diameter strongly suggests the formation of a second corona of nuclei as represented in Figure 14b. The calculation of the minimum seed

diameter needed for promoting the axial growth of such a second corona along the z direction of the considered “1 seed–11 nuclei” aggregate (that is $L \geq L_{\text{CRITIC2}}$) gave a Ss/Ns ratio of 2.76, very close to the experimental measurement of the critical Ss/Ns value of 2.8. This consistent observation thus gives much credit to the oriented aggregation growth mechanism proposed in this paper.

Gold Comparison. For comparison purpose, TEM pictures of the early stage of gold nanoparticles prepared in similar conditions (see the Supporting Information, SI 3) were taken. One minute after the seed introduction, already differentiated and twinned nanoparticles could be observed, proving that the growth of gold nanoparticles is much more rapid than that of palladium. Their facets are bumpy and look very similar with those of palladium nanoparticles formed after 9 min. Although the direct homogeneous nucleation of the gold solution is not realistic (the gold salt solution is stable for hours if no seed is added), the introduction of gold seeds may promote a fast surface secondary nucleation leading to the NCs morphology differentiation, or autocatalyze the appearance of nuclei via gold dismutation and promote a very fast oriented aggregation process similar to the one described in this article. The verification of this mechanism is under progress at the moment.

Conclusion

In this article, we presented the seed-mediated synthesis of well structured palladium nanoparticles of various shapes. The detailed kinetic study (summarized in Figure 15) proved that, at the difference of the well-known seed mediated synthesis of gold nanoparticles,^{41,46} the palladium structuration implies at very short time the oriented aggregation of palladium seeds and palladium nuclei issued from homogeneous nucleation of the palladium salt solution. The mechanism of the oriented aggregation of seeds and nuclei was rationalized via the formation of secondary particles, the geometry of which is not random but depends on local free enthalpy minimization. The different geometries of secondary particles determine the final geometries of well-faceted single, twinned, and pentatwinned nanocrystals. Their dominant growing process seems to be an oriented aggregation at short time, followed by a dominant molecular reduction when palladium concentration is too low to promote homogeneous nucleation. The simple geometrical models presented here allow us to explain why pentatwinned nanorod formation is favored in the presence of seeds. As far as we know, this model is the only one able to explain and predict the evolution of palladium nanorods diameter as a function of seed diameters.

Supporting Information Available: Additional images and information (PDF). This material is available free of charge via the Internet at <http://pubs.acs.org>.